ECS Transactions, 86 (3) 89-101 (2018) 10.1149/08603.0089ecst ©The Electrochemical Society

Using Surface Chemistry to Direct the Deposition of Nano-objects for Electronics

J. K. Hedlund^a, A.A. Ellsworth^{a,c}, and A.V. Walker^{a,b}

One of the major challenges in the practical use of nano-objects is their integration into complex structures in a controlled way. We have developed two promising techniques by which to direct the *in situ* growth of metallic and semiconducting nano-objects. ENDOM, or Electroless Nanowire Deposition on Micropatterned substrates, employs electroless deposition, while SENDOM, or SEmiconductor Nanowire Deposition on Micropatterned substrates, uses chemical bath deposition. In ENDOM nanowire adhesion to the substrate can be controlled using the concentration of bath additives. Using this effect we show that copper nanowires can be transferred to a variety of substrates. After transfer, the nanowires maintain their size, structural integrity, pattern and properties. Using SENDOM, we show that the nanowire formation is controlled by the interaction of a chalcogenide ion with the surface, and consequently is strongly pH dependent.

Introduction

Nano-objects, including nanowires, nanopores, nanorings and nanochannels, have many applications in electronics (1, 2), sensing (3-6), energy conversion (7), optoelectronics (8) and non-linear optics (9). One of the major challenges in the practical use of these structure is their integration into complex functional structures in a predictable and controlled way from the nanoscale to the mesoscale. Currently nano-objects are often produced by complex processes, which are not easily controlled and require multiple lithographic, deposition and etching steps (1-10).

We have recently demonstrated a single *in situ* method by which to create metallic nanoand meso- structures over square-centimeter areas (11-13). ENDOM, or electroless nanowire deposition on micropatterned substrates, employs electroless deposition (ELD) to form nano- and meso- structures. In ENDOM nanostructures are formed at the boundary between two unlike materials if two conditions are met: (a) deposition is kinetically preferred on one of the materials and (b) transport of reactants is favored on the other. In Figure 1, a schematic of the method is shown (11). First, using UV photopatterning an image is created in a hydroxyl terminated self-assembled monolayer (SAM) (SAM1) (step 1). A multi-functional patterned surface is then created by adsorbing a methyl terminated SAM (SAM2) where SAM has photo-oxidized (step 2). The patterned SAM1/SAM2 sample is then immersed in an ELD bath (step 3). ELD processes are REDOX processes which can be employed to deposit a wide range of materials, including metals and semiconductors. In ENDOM, metal ions are reduced by dimethylamine borane (DMAB).

^a Department of Chemistry Biochemistry, University of Texas at Dallas, Richardson, Texas 75080, USA

^b Department of Materials Science and Engineering, University of Texas at Dallas, Richardson, Texas 75080, USA

^c Present address: Physical Electronics, 18725 Lake Drive East, Chanhassen, MN 55317

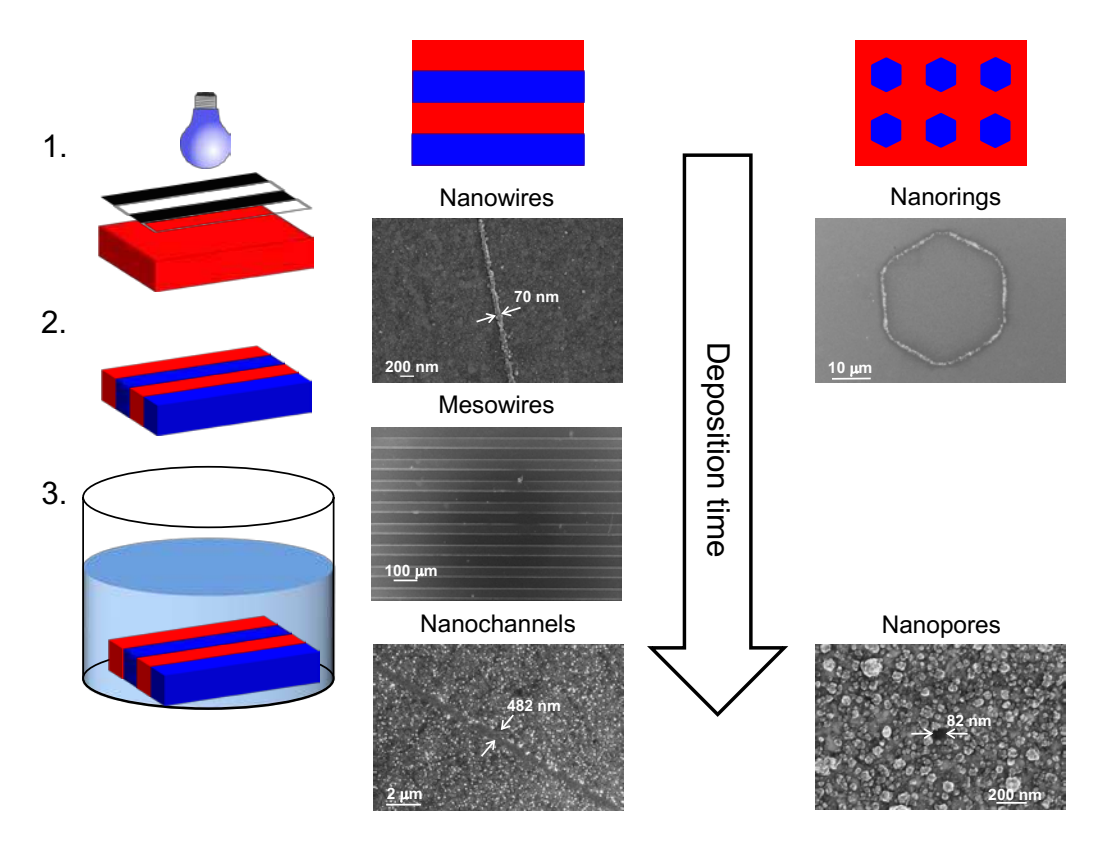


Figure 1. Schematic of electroless nanowire deposition on micropatterned substrates (ENDOM). (1) Using UV photopatterning a pattern is produced in SAM1 (-OH-terminated SAM). (2) In the photooxidized SAM1 areas, SAM2 (-CH₃-terminated SAM) is adsorbed. (3) The sample is then placed in an ELD bath. At the interface between SAM1 and SAM2, nanostructures and mesostructures are electrolessly deposited. Initially nanowires and nanorings form. At longer deposition times, these develop into mesostructures, and eventually nanochannels and nanopores form. Example SEM images of nanowires, mesowires, nanochannels, nanorings, and nanopores are shown. Reprinted with permission from A.A. Ellsworth, A.V. Walker, Langmuir 32 (2016), 2668–2674. Copyright 2016 American Chemical Society.

For example, copper nano-objects are deposited via the following reaction:

$$3Cu^{2+} + (CH_3)_2NHBH_3 + 3H_2O \rightarrow 3Cu + (CH_3)_2NH_2^+ + H_3BO_3 + 5H^+$$
 [1]

Initially copper deposition begins at the interface between –OH and –CH₃ terminated SAMs because DMAB is preferentially adsorbed on the hydrophobic –CH₃ terminated SAM while the transport of the reactants is favored on the hydrophilic –OH terminated SAMs.

In ENDOM, the deposit dimensions are controlled by the nature and concentration of the reagents, bath pH and temperature, and deposition time (11). For example, at a given reaction condition, the deposition time controls the deposit dimensions. Initially nanowires or nanorings are produced (Figure 1). At longer deposition times these nanostructures form mesostructures and eventually nanochannels or nanopores as the deposit nearly fills the –CH₃ terminated SAM area. After formation of the first nanostructure layer, further

patterning/deposition cycles can be employed to assemble complex devices such as cross-bars (data not shown) (14).

In this paper we discuss the effect of the bath additive, triethanolamine (TEOA), on the adhesion of the produced nanostructures. We exploit this result to remove nanowires from the gold substrate so that their electrical properties can be measured. Second, we demonstrate that chemical bath deposition (CBD), an ion exchange reaction, can be employed to produce semiconducting nanowires in a similar process to ENDOM. Finally, we also discuss the effect of the CBD solution pH on the deposit chemistry.

Experimental

Sample Preparation

Gold (99.995%), chromium (99.995%), thiourea (99%), thioacetamide (99+%)and triethanolamine (98+%) were obtained from Alfa Aesar, Inc. (Ward Hill, MA). Copper (II) sulfate pentahydrate (CuSO₄·5H₂O, 98+%), ethylenediaminetetraacetic acid (EDTA) (98%), dimethylamine borane complex (97%), hexadecanethiol (HDT) (99+%), and 16-hydroxy-1-hexadecanethiol (MHL) (99+%) were purchased from Sigma Aldrich, Inc. (St. Louis, MO). Concentrated sulfuric acid (95%) was obtained from BDH Aristar, Inc. (Chester, PA). Sodium hydroxide (\geq 98%, pellets) were purchased from Fisher Chemicals. All reactants were used without further purification. Silicon wafers (\langle 111 \rangle orientation) were purchased from Addison Engineering Inc. (San Jose, CA) and cleaned using RCA SC-1 etch (H₂O:NH₄OH:H₂O₂=5:1:1) for 20 minutes prior to use.

The preparation of self-assembled monolayers (SAMs) has been described in detail previously (15-18). In brief, chromium (\sim 50 Å) and then gold (\sim 1000 Å) were thermally deposited onto freshly etched Si wafers. A well-ordered SAM was formed by immersing the gold substrate into a 1 mM ethanolic solution of the appropriate alkanethiol (MHA, MHL or HDT) for 24 hours at ambient temperature, 21 ± 2 °C. The SAM was then rinsed with copious amounts of ethanol, and dried under N₂ gas.

UV Photopatterning

The MHL or MHA SAMs was UV photopatterned using the procedure described by Zhou and Walker (19). A mask (copper TEM grid of the appropriate pattern, Electron Microscopy Inc., Hatfield, PA) was placed on top of the MHL or MHA SAM (SAM1). The construct was then placed approximately 50 mm from a 500 W Hg arc lamp equipped with a dichroic mirror and a narrow band-pass UV filter (280 to 400 nm) (Thermal Oriel, Spectra Physics Inc., Stratford, CT). It was then exposed to UV light for 3 hours to ensure that the photooxidation of SAM1 was complete. After photooxidation SAM1 was rinsed with ethanol and then immersed in a 1 mM ethanolic solution of a second alkanethiol (HDT or MHL) for 24 hours at ambient temperature. In the areas exposed to UV light the photooxidized SAM1 was displaced by either a –CH3 terminated SAM (HDT) or –OH terminated SAM (MHL) creating a patterned SAM1/SAM2 surface. The patterned substrates were then rinsed with ethanol, dried with N2 gas, and used immediately for deposition.

Electroless Deposition

The standard copper electroless deposition solution ("100 %") was composed of 0.032 M copper (II) sulfate pentahydrate, 0.24 M triethanolamine, 0.037 M EDTA (complexing agent), and 0.067 M dimethylamine borane (DMAB, (CH₃)₂NHBH₃) (reducing agent). To investigate the adhesion of the nanowires, the concentration of triethanolamine was altered, while the concentrations of all other reagents remained constant. Before addition of the reducing agent, DMAB, the pH of the deposition bath was adjusted to 9. The deposition

temperature was 22±1 °C. After deposition each sample was rinsed with DI water and ethanol. The resulting constructs were examined using time-of-flight secondary ion mass spectrometry (TOF SIMS), scanning electron microscopy (SEM) and optical microscopy. Chemical Bath Deposition

The bath was composed of 0.006 M copper(II) sulfate pentahydrate (copper source), 0.012 M EDTA (complexing agent), 0.012 M thiourea or thioacetamide (sulfur source), and 0.012 M sodium hydroxide. To make the deposition solution, copper(II) sulfate pentahydrate was added to DI water, then EDTA and sodium hydroxide were added. The solution was then sonicated for 15 minutes. The pH of the solution was then altered through the addition of sulfuric acid to either pH 12, 11, 10 or 9. Finally, thiourea or thioacetamide was added while the solution was stirred. SAM samples were then immersed in the solution 18 to 24 hours. The bath solution remained at constant pH and temperature during the reaction. After the reaction, the samples were sonicated in deionized water for 2 minutes, rinsed, dried using nitrogen gas, and examined using TOF SIMS, optical microscopy, SEM or x-ray photoelectron spectroscopy (XPS).

Nanowire Transfer

Three different methods were employed to transport the copper nanowires from the SAM substrate. First, copper nanowires were transferred to PMMA films. Spin-coating of PMMA was performed by first dissolving PMMA (average Mw ~996 000 by GPC, Sigma-Aldrich product no.182265) was first dissolved in chlorobenzene with a concentration of 46 mg/ml. The PMMA solution was spin coated at 3,000 rpm to the SAM/Cu nanowire substrate. The sample was cured for 1 minute at 180°C, and the PMMA film lifted from the sample surface using uniform force.

Second, nanowires were transferred to carbon tape by applying ultrasmooth carbon adhesive tabs or double-sided copper tape (Electron Microscopy Inc., Hatfield, PA) to the SAM/Cu substrate. The carbon adhesive tab or tape was then lifted from the SAM surface using uniform lift off force.

Third, nanowires were transferred to Si wafers using heat transfer tape. Double-sided heat transfer tape (HTT) (REVALPHA No. 3195, Nitto Inc., Teaneck NJ) was applied to a freshly etched bare Si wafer. The SAM/Cu nanowire substrate was then placed face down atop the Si/HTT stack. A uniform force of 1 N/mm² was applied to the stack for 10 minutes using a pressure plate. The Si/HTT/Si stack was then heated to 120°C for 10 minutes, allowing the HTT to fall away leaving the nanowires on the Si surface.

X-ray Photoelectron Spectroscopy (XPS)

Photoelectron spectra were measured with a PHI VersaProbe II (Physical Electronics Inc., Chanhassen, MN) equipped with a monochromatic Al K α X-ray source (E $_p$ = 1486.7 eV). Typically, the pressure of the chamber was <5 × 10⁻¹⁰ mbar during analysis. The data were collected using a pass energy of 23.5 eV and an energy step of 0.2 eV. The data were collected at 45° to the normal of the sample surface. The XPS spectra were analyzed using CasaXPS 2.3.16 (RBD Instruments, Inc., Bend, OR) and AAnalyzer 1.07. The binding energies were calibrated using the Au 4f7/2 binding energy (84.0 eV).

Time-of-Flight Secondary Ion Mass Spectrometry (TOF SIMS)

TOF SIMS measurements were performed using an ION TOF IV spectrometer (ION TOF Inc., Chestnut Hill, NY) equipped with a Bi liquid metal ion gun. The instrument consists of a loadlock used for sample introduction, preparation and analysis chambers. The pressure of the preparation and analysis chambers was typically less than 5×10^{-9} mbar. The Bi⁺ primary ions had a kinetic energy of 25 keV and were contained within a ~100 nm diameter probe beam. The primary ion beam was rastered over a $(500 \times 500) \, \mu m^2$ area

during data acquisition. All spectra were acquired using an ion dose of less than 10¹¹ ions cm⁻², which is within the static regime (20).

Scanning Electron Microscopy

SEM images were acquired from a Zeiss Supra 40 Field Emission Scanning Electron Microscope with an image resolution of 1-2 nm. To prevent nanowire charging, a thin film (~60 Å) of gold was sputter coated onto the samples prior to imaging.

The reported wire widths are measured from the SEM image using ImageJ (21). For each nanowire, ten widths were measured along its length, and the average width is reported. The lengths of the nanowires were also measured from the SEM images using ImageJ.

Optical Microscopy

Optical microscopy was performed using a Keyence VHX-2000 digital microscope (Keyence Corporation of America, Itasca IL). Dark field images were obtained from representative samples with 200× magnification.

Electrical Measurements

For the electrical characterization, a Cascade Summit series probe station (Cascade Microtech, Beaverton OR) was used. The probe station allows current measurement down to in the fA range and capacitance as low as tens of fF. The probe station is equipped with a Keithley 4200 semiconductor parameter analyzer (Tektronix Inc., Beaverton OR). Two tungsten probes were placed directly on the individual wires and the voltage was swept from -0.1 V to 0.1 V and the current was recorded.

Results and Discussion

ENDOM: Effect of Additive Concentration on Nanowire Adhesion

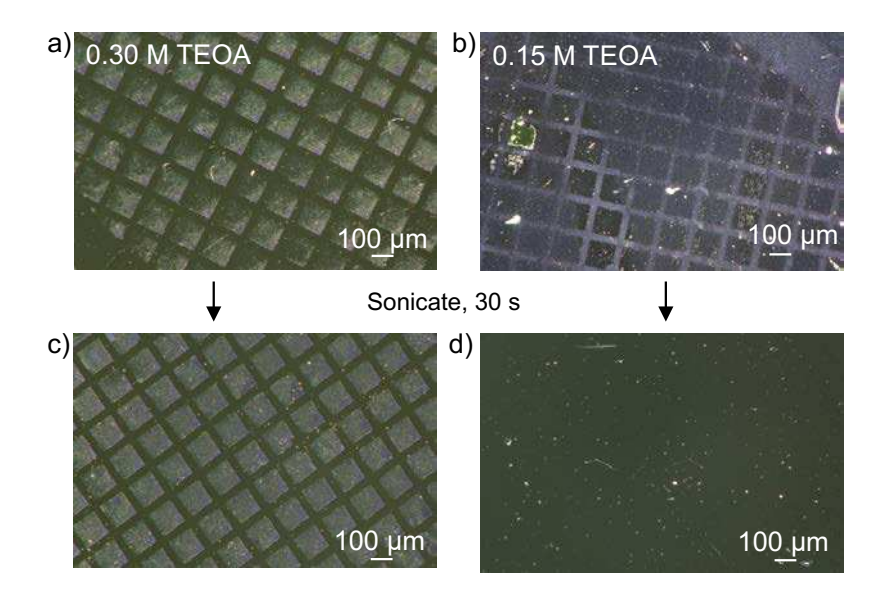


Figure 2. Optical images of –CH₃/–OH patterned SAMs after Cu ELD using a) and c) 100 % (0.30 M) TEOA, and b) and d) 50 % (0.15 M) TEOA. a) and c) Before sonication. b) and d) After sonication in water for 30 s. Deposition conditions: 0.032 M copper (II) sulfate pentahydrate, 0 0.037 M EDTA, 0.067 M DMAB, 22±1 °C, pH 9, deposition time 30 min.

Figure 2 shows optical images after copper electroless deposition using 0.15 M (50 %) and 0.3 M (100 %) triethanolamine (TEOA) on a patterned –CH₃ and –OH terminated SAM before and after sonication of the sample in water. We note that we have previously observed that the concentration of bath additives changes deposition rates and selectivity of the copper deposition (22). Prior to sonication using 100 % TEOA copper is deposited in the methyl terminated SAM areas (Figure 2a: "square areas"). In contrast to 100 % TEOA, using 50 % TEOA the deposit selectivity is switches, and copper is formed in the hydroxyl terminated areas (Figure 2b: "bars"). Using 50 % TEOA, after sonication most of the deposited copper is removed from the surface. In contrast, using 100 % TEOA the deposited copper adheres to the substrate even after sonication.

To further confirm the dependence of Cu adhesion on triethanolamine concentration, the following experiment was performed. A mixed SAM was synthesized with a 1:1 ratio of –OH to –CH3 terminated SAMs. In a mixed SAM, the terminal groups are randomly distributed across the Au substrate and so there are many more –OH/–CH3 boundaries to serve as Cu nucleation sites. Since the SAMs are randomly distributed copper nanoparticles are formed (Figure 3). Interestingly, using 50% TEOA the nanoparticle size appears to be more uniform than those deposited from a bath containing 100 % TEOA. Copper tape was then applied and removed using even pressure and a consistent lift off angle and speed. After tape removal, most of the copper nanoparticles remain on the surface using 100 % TEOA (Figure 3a). Using 50% TEOA the copper nanoparticles appear to be removed from the surface after application of the tape (Figure 3b). Further, TOF SIMS data confirm that most of the deposited copper has been removed (data not shown).

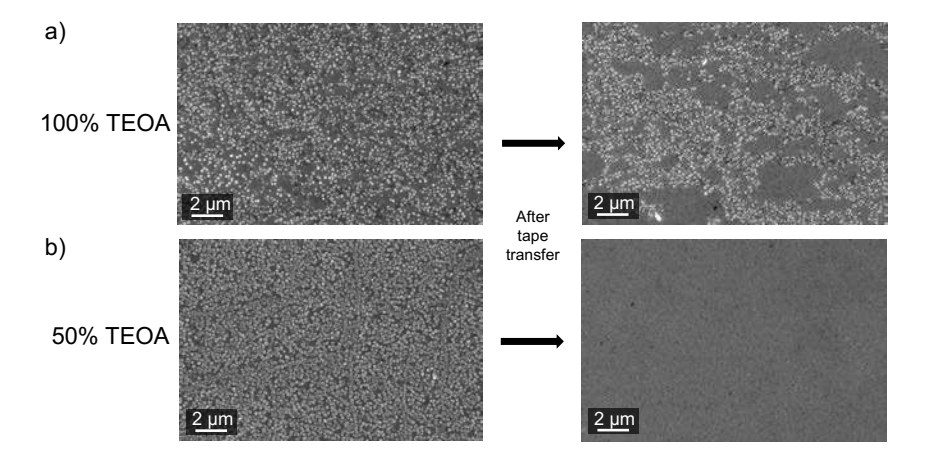


Figure 3. SEM images of a mixed MHL/HDT SAM surface after copper deposition before and after tape removal using a) 100 % (0.3 M) TEOA and b) 50% (0.15 M) TEOA . Deposition conditions: 0.032 M copper (II) sulfate pentahydrate, 0 0.037 M EDTA, 0.067 M DMAB, 22 ± 1 °C, pH 9, deposition time 15 min.

TOF SIMS was also employed to investigate the interaction of TEOA at the interface of the patterned –OH/–CH₃ SAM surface during the initial nanowire formation. In the mass spectra cluster ions of the form [Cu₂(MHL)(HDT)OH]⁻ (MHL = -S(CH₂)₁₅CH₂OH; HDT = -S(CH₂)₁₅CH₃) are observed indicating that copper initially deposits at the –OH/–CH₃ terminated SAM interface (Figure 4). We attribute the –OH functional group in the ion to the TEOA additive present in the solution. As the concentration of TEOA decreases, there is a significant reduction in the [Cu₂(MHL)(HDT)OH]⁻ ion intensity and simultaneously

nanowire adhesion. This suggests that the triethanolamine mediates the adhesion of the deposited copper with the SAM surface.

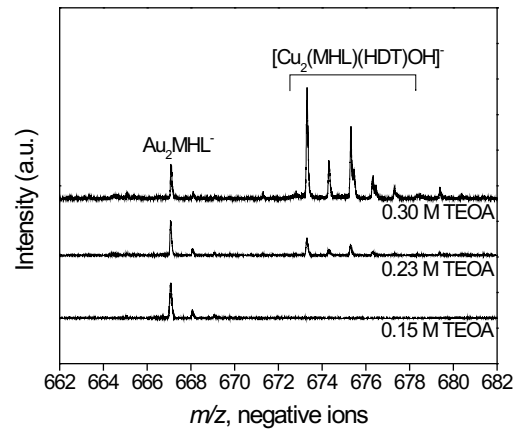


Figure 4. High resolution negative ion spectra centered at m/z 672 after copper electroless deposition on patterned –OH/–CH₃ terminated SAMs as the triethanolamine (TEOA) concentration is varied from 50% (0.15 M) to 100% (0.30 M). Deposition conditions: 0.032 M copper (II) sulfate pentahydrate, 0 0.037 M EDTA, 0.067 M DMAB, 22±1 °C, pH 9, deposition time 10 min.

ENDOM: Nanowire Transfer to Insulating Substrates and Preliminary Electrical Characterization

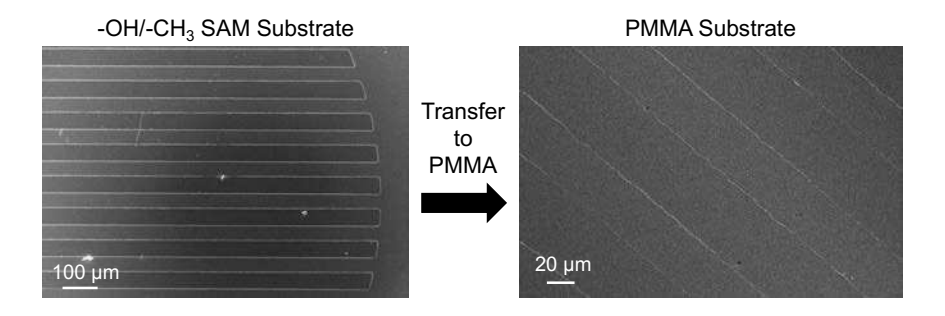


Figure 5. SEM images of Cu nanowires deposited on a parallel bar –CH₃/–OH patterned SAM surface using 50% (0.15 M) TEOA and then transferred to PMMA.

Since [TEOA] alters the adhesion of the copper nanowires on patterned –OH/–CH₃ terminated SAMs, three different transfer methods were developed. First, copper nanowires were transferred to poly (methyl methacrylate). PMMA is a transparent, strong, flexible, and biocompatible polymer (23-25). After spin coating the PMMA solution and allowing it to cure, the PMMA substrate was removed from the gold substrate. In Figure 5 it can clearly be seen that the nanowires have transferred to the PMMA film and maintained their structural integrity, and original dimensions and pattern. The nanowires were also transferred to carbon tape. Similar to PMMA, after carbon tape is applied to the substrate and lifted off, the nanowires are transferred to the carbon tape. Again the nanowires maintained their original dimensions and the pattern is preserved after liftoff (data not shown).

However, using these methods it was not possible to perform a second transfer of the nanowires to a technologically substrate such as silicon. We therefore developed a third method by which to transfer the nanowires using heat transfer tape (HTT). Heat transfer

tape is thermally conductive and electrically insulating. When applied to the substrate (Figure 6a) for 10 minutes with 1 N/mm² force, the Cu nanowires were lifted from the patterned SAM surface (Figure 6b). The nanowires were then transferred to another substrate using the following procedure. The HTT/nanowire sample was heated to above 120°C. At these temperatures the HTT loses its adhesive strength. Thus, the nanowires can be removed from the HTT and transferred to a target substrate, such as a Si surface (Figure 6c).

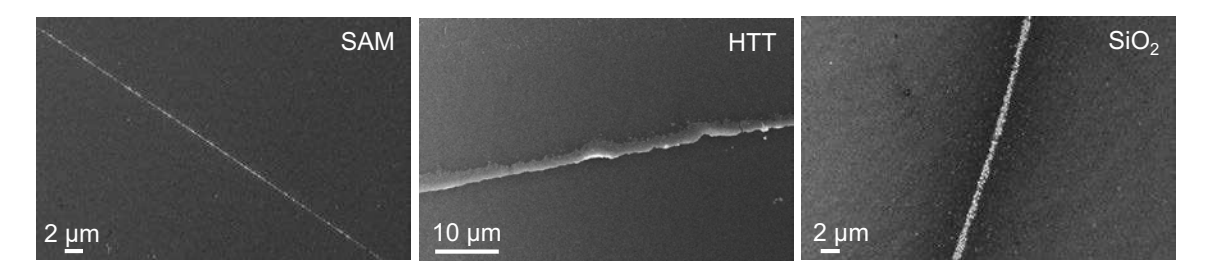


Figure 6. SEM images of Cu nanowire formed on a patterned –CH₃/–OH SAM substrate ("SAM"), then transferred to HTT ("HTT"), and finally from the HTT to SiO₂ ("SiO₂").

Preliminary electrical measurements of large copper nanowires adhered to the HTT were performed. The I-V behavior for all the nanowires measured was ohmic. From these measurements the electrical conductivity of the nanowires was calculated. Since the deposited nanowires are polycrystalline and small, it was expected that the resistivity of the nanowire is larger than for bulk copper, $\rho_0 = 1.9 \times 10^{-8} \Omega m$ (26-30). This is because there is inelastic scattering of electrons at the wire surfaces (31, 32), and reflection of the electrons at the grain boundaries (27). To account for these factors, Steinhögl and coworkers (30) derived the following equation for nanowires with a rectangular cross-section:

$$\rho = \rho_0 \left\{ \frac{\frac{1}{3}}{\left[\frac{1}{3} - \frac{\alpha}{2} + \alpha^2 - \alpha^3 \ln\left(1 + \frac{1}{\alpha}\right)\right]} + \frac{3}{8}C(1 - p)\frac{1 + AR}{AR}\frac{\lambda}{w} \right\} \text{ with } \alpha = \frac{\lambda}{d}\frac{R}{1 - R}$$
 [2]

where AR is the wire aspect ratio (ratio of wire height to wire width), C is a geometrical parameter (C = 1.2 for nanowires with rectangular cross-sections), w is the width of the nanowire, d is the average grain size (d = 200 nm (11)), λ is the electron mean free path (λ = 40 nm at room temperature (30)), R is the reflection coefficient for grain boundaries and is assumed to be 0.9 (29), and p is the fraction of electrons that are specularly scattered from the wire surfaces and is assumed to be 0.5 (30). Preliminary results for the measured and calculated wire resistivities are shown in table 1.

TABLE I. Experimentally measured resistivities for two Cu wires of different widths compared with calculated resistivities.

Wire Thickness (nm)	Wire Width (nm)	Experimental Resistivity (Ωm)	Calculated Resistivity (Ωm)
100	756	1.26×10^{-6}	6.75×10^{-8}
100	756	2.99×10^{-7}	6.75×10^{-8}

We note that Equation 2 predicts a resistivity that is lower than the experimentally measured resistivities by a factor of less than 20. Previously it has also been reported that higher experimental resistivities are measured than are calculated for polycrystalline nanowires (2, 29, 30). The differences in the experimental and calculated resistivities can

be attributed to several reasons. First, the specular scattering and reflection coefficients are assumed to be constants but may vary with nanowire size (30). Second, the contact resistance of the probes may also alter the measured resisitivities.

SEmiconductor Nanowire Deposition on Micropatterned Substrates (SENDOM): CuxS Nanowire Formation

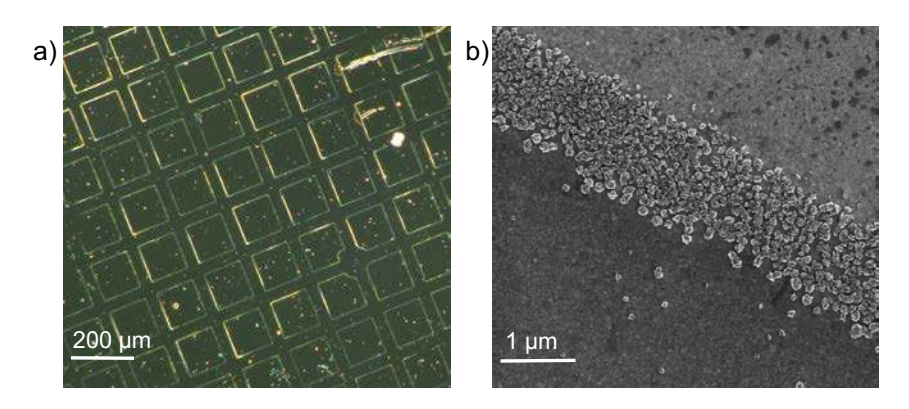


Figure 7. a) Optical and b) SEM images of Cu_xS nanowires formed at the interface of –OH and –COOH terminated SAMs. Deposition: bath pH 12, deposition time 24 h.

A second solution-based deposition method, chemical bath deposition (CBD), can be employed to deposit semiconducting nanowires. We term this method SEmiconductor Nanowire Deposition On Micropatterned substrates (SENDOM). In SENDOM the interaction of a chalcogenide ion with the sample surface is employed to control the nanostructure formation. The process is similar to that shown in Figure 1. First, a micropatterned –OH/ –CH₃ or –COOH/–CH₃ or –COOH/–OH SAM surface is created. The sample is then immersed into a bath with the appropriate reagents for Cu_xS CBD. In a similar manner to ENDOM, a nanowire will form on micropatterned -OH/-CH₃ or -COOH/-CH₃ SAM surfaces at short deposition times because deposition is faster on the -CH₃ terminated surface but transport of reactants is preferred to the hydrophilic SAM surface, -COOH or -OH terminated SAM. In contrast to ENDOM, nanowires will also form at the interface of micropatterned -COOH/-OH SAMs due to the interaction of the chalcogenide ions with the -COOH terminated SAM. Figure 7 displays optical and SEM images of Cu_xS nanowires obtained. The formed nanowires also follow complex shapes, such as a right-angled bend, and are ultralong (centimeters) because they form at the interface between the two dissimilar SAM surfaces.

CBD a controlled ion exchange reaction is used to deposit thin films of II-VI semiconductors and other materials (33). Typically in CBD reactions both the concentration of the cation and chalcogenide ion are controlled. In this study, copper sulfide was deposited using the following (unbalanced) reaction equation (33, 34):

$$\begin{array}{c} Cu^{2^{+}} + EDTA^{4^{-}} \rightarrow [Cu(EDTA)]^{2^{-}} & [3] \\ SC(NH_{2})_{2} + OH^{-} \rightarrow CN_{2}H_{2} + H_{2}O + HS^{-} & [4] \\ C_{2}H_{5}NS + 2OH^{-} \rightarrow CH_{3}COO^{-} + NH_{3} + HS^{-} & [5] \\ HS^{-} + OH^{-} \rightarrow S^{2^{-}} + H_{2}O & [6] \\ Cu^{2^{+}} + S^{2^{-}} \rightarrow CuS & [7] \\ 2Cu^{+} + S^{2^{-}} \rightarrow Cu_{2}S & [8] \end{array}$$

To control the concentration of "free" copper ions in solution, copper ions present in solution are complexed with ethylenediaminetetraacetic acid (EDTA) (equation 3).

Thiourea (equation 4) or thioacetamide (equation 5) then with hydroxide ions present in the bath to form bisulfide ions (HS $^{-}$) which subsequently decompose to sulfide ions (S $^{2-}$) (equation 6). Finally, "free" copper ions can combine with the formed sulfide ions (S $^{2-}$) to precipitate either cupric sulfide (CuS) or cuprous sulfide (Cu₂S).

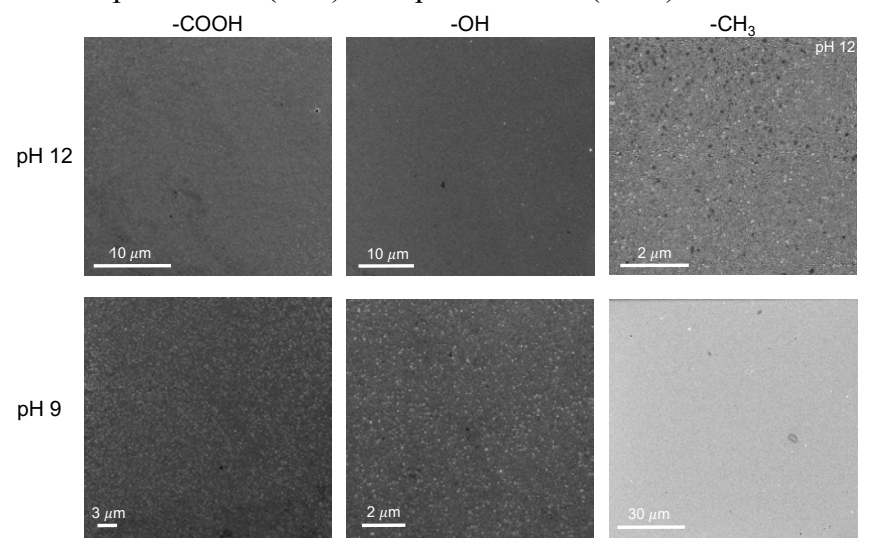


Figure 8. SEM images after Cu_xS deposition for 18 h. on –COOH, –OH and –CH₃ terminated at bath pH 9 and pH 12. Deposition conditions: room temperature, sulfur source – thioacetamide.

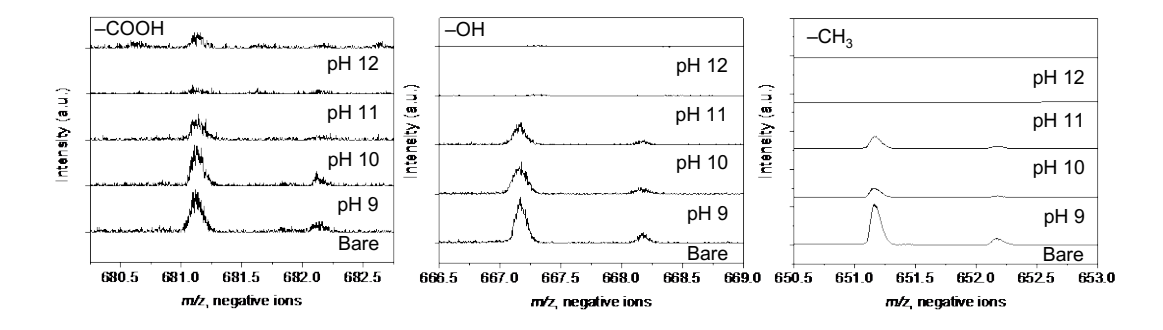


Figure 9. High resolution negative ion spectra centered at the Au₂M⁻ region after Cu_xS deposition for 18 h on –COOH (M = -S(CH₂)₁₅COOH; m/z 681.2), –OH (M = -S(CH₂)₁₅CH₂OH; m/z 667.2) and –CH₃ (M = -S(CH₂)₁₅CH₃; m/z 651.2) terminated SAMs as the bath pH is varied from pH 9 to pH 12.

The Cu_xS CBD process is strongly pH dependent. At room temperature and pH 9, SEM images show that copper sulfide deposits on both the –OH and –COOH terminated SAMs but not on –CH₃ terminated SAMs after 18 hours (Figure 8). However, at pH 12 deposition is preferred on –CH₃ SAMs; little deposition is observed on –OH and –COOH SAMs. Further, in agreement with the SEM, the intensity of the molecular cluster ions, Au₂M⁻, for the –COOH, –OH and –CH₃ SAMs indicate that the copper sulfide deposition changes with pH (Figure 9). Using thioacetamide as the sulfur source, for –COOH terminated SAMs the ion intensity of Au₂M⁻ decreases from pH 9 to pH 11 indicating that more Cu_xS is deposited as the pH increases. However, at pH 12 the intensity of Au₂M⁻ increases indicating that less Cu_xS has deposited. For –OH terminated SAMs, from pH 9 to pH 11 the ion intensity of Au₂M⁻ decreases but a small intensity of Au₂M⁻ is observed at pH 12.

These results suggest that the Cu_xS does not fully cover the SAM. In contrast, for $-CH_3$ terminated SAMs as the bath pH increases the ion intensity of Au_2M^- decreases significantly and no molecular cluster ions are observed after deposition at pH 11 and pH 12 indicating that the SAM is completely covered by the deposited Cu_xS .

The preferential deposition of copper sulfide on -CH₃ terminated SAMs can be explained in the following way. As the pH of the bath increases, the solution concentration of S²- increases from $\sim 5 \times 10^{-9}$ M at pH 9 to $\sim 5 \times 10^{-6}$ M at pH 12 (33). The pKa of hexadecanoic acid (palmitic acid) is $\sim 8.5-8.8$ (35). Thus, as the pH of the deposition bath increases, it is likely that exponentially increasing numbers of the terminal groups in the -COOH terminated SAMs deprotonate. These deprotonated SAM terminal groups form carboxylate/Cu(II) complexes which serve as the nucleation sites for copper sulfide deposition. Thus from pH 9 to 11 more copper sulfide is deposited. However, at pH 12 the carboxylic acid terminated SAM is almost fully deprotonated (99.99 %). Since the association constant of Cu²⁺ with carboxylate groups is relatively low (< 1000) (36, 37), the repulsive interaction between the S²- ions and the COO terminal dominates the CBD process and the reaction slows. Similarly, The C-OH terminal bond of the hydroxylterminated SAM is covalent and polar with the –OH group having a small negative charge $(\delta -)$. There is a smaller repulsive interaction between the S²⁻ ions, and so the reaction slows slightly as the pH increases. In contrast, the C-H bonds of the methyl terminal group are not polar. Thus, S²- adsorption is preferred on the -CH₃-terminated SAM and as the concentration of the S²- ions increases with pH, the deposition of copper sulfide increases.

Our data also indicates that the bath pH changes the type of copper sulfide deposited. Using XPS, the modified Auger parameter for Cu (38) indicates that for all SAMs studied cupric sulfide is deposited if thioacetamide is employed as the sulfur source as the bath pH changes. However, using thiourea as the sulfur source, the XPS photoelectron intensities indicate that the deposition is slower leading to changes in the chemistry of copper sulfide deposited. For –OH and –CH₃ terminated SAMs, the modified Auger parameter indicates that cupric sulfide is deposited as the bath pH increases (38). However above pH 10, on –COOH terminated SAMs cuprous sulfide is deposited. We are currently performing further studies to understand this effect.

Conclusions

We have introduced two promising new techniques by which to direct the *in situ* growth of metallic and semiconducting nano-objects. ENDOM, or Electroless Nanowire Deposition On Micropatterned substrates, employs electroless deposition (ELD) to form metallic nanostructures on substrates. SENDOM, or SEmiconductor Nanowire Deposition on Micropatterned surfaces, uses chemical bath deposition (CBD) to deposit semiconductor nanowires. Using these processes we have demonstrated the production of nanowires (diameters < 100 nm), mesowires (100 nm < diameter < ~3000 nm), nanorings, nanopores and nanochannels.

In Cu ENDOM the adhesion of the deposited nanostructures is dependent on the concentration of TEOA, an ELD bath additive. By reducing the concentration of TEOA, the copper nanowires can be transferred to other substrates, such as PMMA and silicon. After transfer, the nanowires maintained their size, structural integrity and relative position (pattern). Preliminary electrical measurements indicate that the deposited copper nanowires are conductive.

In Cu_xS SENDOM, the deposition occurs at the interface of –COOH and –CH₃, –OH and –CH₃, and –COOH and –OH SAMs. On micropatterned –OH/–CH₃ or –COOH/–CH₃

SAM surfaces Cu_xS nanowires form at short deposition times because deposition is faster on the –CH₃ terminated SAM surface but transport of reactants is preferred to the hydrophilic SAM surface, –COOH or –OH terminated SAM. Nanowires also form at the interface of micropatterned –COOH/–OH SAMs due to the interaction of the chalcogenide ions with the –COOH terminated SAM.

Acknowledgments

The authors gratefully acknowledge support from the National Science Foundation (CHE 1213546 and CHE 1708258). The authors would also like to thank Rohan Joshi, Jevalyne Vienes, Hannah Ramsaywak, Cheyenne Beaver and Kasey Berger for their help.

References

- 1. J. Chen, M. A. Reed, A. M. Rawlett, and J. M. Tour, *Science*, **286**, 1550 (1999).
- 2. E. J. Menke, M. A. Thompson, C. Xiang, L. C. Yang, and R. M. Penner, *Nat. Mater.*, **5**, 914 (2006).
- 3. F. Favier, E. C. Waiter, M. P. Zach, T. Benter, and R. M. Penner, *Science*, **293**, 2227 (2001).
- 4. B. N. Miles, A. P. Ivanov, K. A. Wilson, F. Doğan, D. Japrung, and J. B. Edel, *Chem. Soc. Rev.*, **42**, 15 (2013).
- 5. C. Dekker, *Nat. Nanotechnol.*, **2**, 209 (2007).
- 6. W. Reisner, J. N. Pedersen, and R. H. Austin, *Rep. Prog. Phys.*, **75**, 106601 (2012).
- 7. T. J. Kempa, R. W. Day, S.-K. Kim, H.-G. Park, and C. M. Lieber, *Energ. Environ. Sci.*, **6**, 719 (2013).
- 8. A. R. Halpern and R. M. Corn, *ACS Nano*, 7, 1755 (2013).
- 9. J. Junesch and T. Sannomiya, ACS Appl. Mater. Interfaces, 6, 6322 (2014).
- 10. A. V. Whitney, B. D. Myers, and R. P. Van Duyne, *Nano Lett.*, **4**, 1507 (2004).
- 11. A. A. Ellsworth and A. V. Walker, *Langmuir*, **32**, 2668 (2016).
- 12. A. A. Ellsworth, K. Borner, J. Yang, and A. V. Walker, ECS Trans., 58, 1 (2014).
- 13. Z. Shi and A. V. Walker, *Langmuir*, **27**, 11292 (2011).
- 14. A. A. Ellsworth, PhD Thesis, The University of Texas at Dallas, 2017.
- 15. R. G. Nuzzo, L. H. Dubios, and D. L. Allara, *J. Am. Chem. Soc.*, **112**, 558 (1990).
- 16. M. D. Porter, T. B. Bright, D. L. Allara, and C. E. D. Chidsey, *J. Am. Chem. Soc.*, **109**, 3559 (1987).
- 17. G. L. Fisher, A. E. Hooper, R. L. Opila, D. L. Allara, and N. Winograd, *J. Phys. Chem. B*, **104**, 3267 (2000).
- 18. G. L. Fisher, A. V. Walker, A. E. Hooper, T. B. Tighe, K. B. Bahnck, H. T. Skriba, M. D. Reinard, B. C. Haynie, R. L. Opila, N. Winograd, and D. L. Allara, *J. Am. Chem. Soc.*, **124**, 5528 (2002).
- 19. C. Zhou and A. V. Walker, *Langmuir*, **22**, 11420 (2006).
- J. C. Vickerman and D. Briggs, eds., <u>TOF-SIMS</u>: <u>Materials Analysis by Mass Spectrometry</u>. 2nd Edition, IM Publications LLP and SurfaceSpectra Limited, Chichester and Manchester UK, 2013.
- 21. https://imagej.nih.gov/ij/download.html, accessed 06/22/2018 11.00 am.
- 22. A. A. Ellsworth and A. V. Walker, *Langmuir*, **34**, 4142 (2018).
- 23. I.-K. Kang, B. K. Kwon, J. H. Lee, and H. B. Lee, *Biomaterials*, 14, 787 (1993).
- 24. P. Gupta, C. Elkins, T. E. Long, and G. L. Wilkes, *Polymer*, **46**, 4799 (2005).

- 25. L. Antl, J. Goodwin, R. Hill, R. H. Ottewill, S. Owens, S. Papworth, and J. Waters, *Colloids Surf.*, **17**, 67 (1986).
- 26. A. Bietsch and B. Michel, *Appl. Phys. Lett.*, **80**, 3346 (2002).
- 27. A. F. Mayadas and M. Shatzkes, *Phys. Rev. B: Condens. Matter*, 1, 1382 (1970).
- 28. G. Reiss, J. Vancea, and H. Hoffmann, *Phys. Rev. Lett.*, **56**, 2100 (1986).
- 29. W. Steinhögl, G. Schindler, G. Steinlesberger, and M. Engelhardt, *Phys. Rev. B: Condens. Matter*, **66**, 075414 (2002).
- 30. W. Steinhögl, G. Schindler, G. Steinlesberger, M. Traving, and M. Engelhardt, *J. Appl. Phys.*, **97**, 023706 (2005).
- 31. K. Fuchs, Math. Proc. Camb. Philos. Soc., 34, 100 (1938).
- 32. E. H. Sondheimer, *Adv. Phys.*, **50**, 499 (2001).
- 33. G. Hodes, *Chemical Solution Deposition of Semiconductor Films*, Marcel Dekker, Inc., New York, Basel, 2002.
- 34. A. E. Martell and R. M. Smith, *Critical Stability Constants*, Plenum Press, New York, 1974.
- 35. J. R. Kanicky and D. O. Shah, *J. Colloid Interface Sci.*, **256**, 201 (2002).
- 36. L. G. Sillen, ed., <u>Stability constants of metal-ion complexes : Section I: Inorganic ligands</u>, The Chemical Society, London, 1964.
- 37. J. W. Bunting and K. M. Thong, Can. J. Chem., 48, 1654 (1970).
- 38. NIST X-ray Photoelectron Spectroscopy Database, NIST Standard Reference Database Number 20, National Institute of Standards and Technology, Gaithersburg MD, 20899 (2000), doi:10.18434/T4T88K, (retrieved 06/22/2018).